Linking carbon and nitrogen mineralization with microbial responses to substrate availability — the DECONIT model

Arjan M. G. de Bruijn · Klaus Butterbach-Bahl

Abstract Simulation of decomposition and inorganic nitrogen release in complex biogeochemical models can be based on different principles. A major problem is the link between carbon and nitrogen mineralization and a description of microbial growth dynamics in dependence of a suite of possible substrates. This contribution considers a first order decomposition model with several carbon pools and one nitrogen pool to investigate how the decomposition of plant types and mineralization of nitrogen is related to carbon quality. The model structure assumes that nitrogen is mobilised with the rate at which the lignin compounds decompose. The decomposition module is coupled with microbial dynamics by adjusted Michaelis Menten equations that relate microbial growth to the availability of various substrates. The model was calibrated using Markov Chain Monte Carlo (MCMC) applied to measured litter remnants, concentrations of lignin, cellulose and nitrogen from 30 in situ incubations of foliage litters. Additionally, data from a laboratory incubation experiment were used to analyse the formation of microbial biomass, dissolved organic

nitrogen, ammonium (NH_4^+) and microbial respiration. Parameter sensitivity was analysed according to the rate of acceptance of various settings in the MCMC calibration chain. The most important parameters for the decomposition process were the decomposition rate of lignin, and the temperature response parameter Q_{10}. The most important parameters for the formation of microbial biomass, dissolved organic nitrogen, ammonium and microbial respiration, were the potential growth rate of the microbial population and the rate of microbial decay. Estimated optimal decomposition rates for field experiments are 0.003 ± 0.002 d^{-1} for lignin like compounds, 0.006 ± 0.004 d^{-1} for cellulose like compounds and 0.0286 ± 0.052 d^{-1} for solutes. The temperature response parameter Q_{10} is 3.2 ± 0.6 and the optimum decomposition temperature is $28.1 \pm 4.3°C$. Important model parameters on microbial biomass and nitrification are the maximum microbial growth rate $\mu_{MAX}=0.13 \pm 0.82$ gC_{mic} $gC_{mic}^{-1}d^{-1}$ or the rate of microbial decay $D=0.006 \pm 0.014$ gC_{mic} $gC_{mic}^{-1}d^{-1}$. The model performance was tested for independent datasets. Generally, correlations between modelled and measured values, expressed in R^2, were high for the remaining tissue dry weight, or concentrations of lignin, cellulose and solutes or organic nitrogen ($R^2>0.84$). Due to uncertainties in measurements of DON and NH_4^+ concentrations, microbial biomass or basal respiration and significant site variability in these parameters, the model performance for these parameters as expressed as R^2 was somewhat lower, but

A. M. G. de Bruijn · K. Butterbach-Bahl (✉)
Karlsruhe Research Centre,
Institute for Meteorology and Climate Research,
Atmospheric Environmental Research (IMK-IFU),
Kreuzeckbahnstr. 19,
82467 Garmisch-Partenkirchen, Germany
e-mail: Klaus.Butterbach-Bahl@imk.fzk.de

statistically highly significant, and in the range of 0.1-0.96.

Introduction

Understanding of feedbacks of climate change on biosphere-atmosphere exchange processes and ecosystem carbon and nitrogen stocks is of outmost importance in order to improve climate change predictions. The magnitude of carbon stored in terrestrial ecosystems, and here mainly in soils, is approx. 2.5–3 times higher as compared to the atmospheric CO_2 pool (IPCC 2007). Soil CO_2 emissions are one of the major sources for atmospheric CO_2 on a global scale (Houghton et al. 1998; Raich and Schlesinger 1992). Soil CO_2 emissions originate on the one hand from decomposition of organic material (heterotrophic respiration) and on the other hand from plant root (autotrophic) respiration. Climate change, i.e. increases in temperature and changes in the amount and distribution of rainfall, will affect soil carbon stocks and soil respiration, with soil respiration being one of the major biosphere feedbacks to global climate change (Cox et al. 2000; Prentice et al. 2001). Therefore, it is utmost importance to improve the description of carbon and nitrogen decomposition and respiration in biogeochemical models, which are increasingly used to simulate biosphere feedbacks to global changes (Kirschbaum 2000; Lenton and Huntingford 2003; Sitch et al. 2008). Berg et al. (1993) stated that the decomposition of organic material is mainly driven by temperature and moisture. Such an explanation somewhat neglects the importance of substrate quality, which has been shown to be of decisive importance by e.g. Cornwell et al. (2008). Still some biogeochemical models do not account explicitly for substrate quality. Such models, as .e.g. the widely used PnET-N-DNDC (Li et al. 2000) and the COUP model (Jansson and Karlberg 2004), are using conceptional pools with defined C:N ratios and pool specific decomposition rates to mimic decomposition and its dependence from changes in environmental conditions such as temperature and moisture. Partitioning of litter into different pools is done e.g. in PnET-N-DNDC on the basis of C:N ratios (Li et al. 2000), but does not depend on tissue concentrations of lignin, cellulose or soluble (e.g. sugars). This has some disadvantages. In PnET-N-DNDC, litter with a narrow C:N ratio will decompose faster and nitrogen will be mineralised faster than carbon. Even when the litters may decompose faster however, nitrogen release seems to be closely coupled to lignin decomposition. This lignin effect is discussed to be due to the physical protection of nitrogen compounds by large lignin structures (Berg and Claugherty 1978; Berg and Ekbohm 1991; Cooke and Whipps 1993; Coûteaux et al. 1995; Fioretto et al. 2005). However, such a protection mechanism is not considered in models such as PnET-N-DNDC or COUP, so that in consequence nitrogen release rates during decomposition are chronically overestimated. Although the biogeochemical model CENTURY/ DAYCENT (Parton et al. 1998) structures its litter pools according to measurable tissue concentrations of lignin and other compounds, it does not account for such a physical protection mechanism either. Again this may result in an overestimation of nitrogen release rates.

Another shortcome in current biogeochemical models in simulating soil carbon and nitrogen turnover and, thus, also e.g. microbial CO_2 production or nitrate leaching, is related to microbial growth responses to changes in soluble carbon and nitrogen concentrations. Numerous approaches relate microbial growth rates to concentrations of dissolved organic carbon (DOC) and inorganic nitrogen. The PnET-N-DNDC model (Li et al. 2000), for example, includes the combined effect of nitrogen and carbon substrate availability for microbial growth by calculating an overall growth rate reduction factor (f_s) from a dissolved organic carbon (f_{DOC}) and inorganic nitrogen (f_N) factors.

$$f_s = \frac{2.0}{1.0/f_{DOC} + 1.0/f_N} \qquad (1)$$

In this approach the DOC response factor f_{DOC} is calculated by a common Michaelis-Menten (MM) formulation (not shown), whereas the nitrogen response factor f_N is calculated by a MM saturation dependency which considers actual inorganic nitrogen concentrations:

$$f_N = \frac{NO_3^- + NH_4^+}{K_N + NO_3^- + NH_4^+} \qquad (2)$$

Such a formulation has the disadvantage that the rate of microbial growth is related with the *sum* of

possible sources for microbial growth, here NO_3^- and NH_4^+, but does not relate to the availability of *particular* sources. This means that the relative contributions of NO_3^- and NH_4^+ to microbial assimilation of nitrogen are fixed in the model code. For example, even if NO_3^- concentrations are high, microbes may still be simulated to preferentially grow on NH_4^+. As a consequence microbial growth is often unrealistically limited if one of the nitrogen sources is short in supply, even though the other source may be abundantly available.

To overcome the mentioned shortcomes in carbon and nitrogen dynamics in existing biogeochemical models we explored an alternative formulation for decomposition and soil microbial nitrogen dynamics which considers effects of plant tissue concentrations of lignin and other compounds on decomposition and which relates microbial growth to individual nitrogen substrates. Finally, we applied the model to various published field and laboratory experiments in order to test its capability to simulate observed trends in organic matter decomposition.

Materials and methods

DECONIT model description

In the framework of this study we developed a new decomposition model, which is intended to be used as a decomposition module in more complex biogeochemical models, which are capable to simulate all ecosystem carbon and nitrogen fluxes. The decomposition model was called DECONIT to illustrate the close link between decomposition and nitrification. Our model contains three litter pools for carbon, and one litter pool for nitrogen (Fig. 1). The total number of pools is smaller than commonly used. For example the decomposition module in the PnET-N-DNDC model (Li et al. 2000) contains seven litter pools that contain carbon and nitrogen according to a fixed ratio. Similarly, decomposition in the COUP model is modelled by using a recalcitrant and a labile litter pool, but with individual and dynamically calculated nitrogen concentrations (Jansson and Karlberg 2004).

DECONIT contains dissolved organic nitrogen (DON) and DOC as well as three species of inorganic nitrogen: NH_4^+, nitrite (NO_2^-) and NO_3^-. It further uses a microbial pool that contains both carbon and

nitrogen. DECONIT has two sinks for carbon (CO_2 and humus), and one sink for nitrogen (humus). The litter pools lignin ($i=1$), cellulose ($i=2$) and solutes ($i=3$) are understood as aggregates that include tissues with similar structure. Hence, cutin is part of the lignin pool and hemicelluloses are part of the cellulose pool. Decomposition of the litters is described as a function of ambient temperature and a compound-characteristic potential decomposition rate:

$$\frac{\delta L_i}{\delta t} = \tau \cdot m \cdot K_i \cdot L_i \tag{3}$$

where K_i is the potential decomposition rate of a litter pool L_i, corrected for temperature by a factor τ, and for moisture by a factor m, and t is the time in days (please note that all notations are provided in Table 1). There are indications that particular components may differ in their response to temperature (e.g. Coûteaux et al. 2002). For reasons of parsimony however, we did not include such differentiation in the model e.g. we feel that including two (Q_{10} estimations) or even four (Q_{10} and optimum temperatures T_{OPT}) additional model parameters would increase model complexity too much. The temperature correction factor is calculated according to:

$$\tau = Q_{10}^{(T-TOPT/10)} \tag{4}$$

The estimated daily ambient temperature is estimated with a minimal temperature model from the average annual temperature, the temperature spread and the assumed sinusoidal shape of temperature seasonality:

$$T = \overline{T} - T_{spread}$$
$$\cdot \sin\left(\left(Jday - \frac{1}{4} \cdot 365\right) \cdot \frac{2.0\pi}{365}\right) \tag{5}$$

where $\overline{T}$ is the average annual temperature, T_{spread} is the difference between the maximum and minimum temperature during the year and $Jday$ is the day, counting since January 1. A moisture dependent decomposition rate reduction factor is calculated according to:

$$m = P/ET_0 \tag{6}$$

Where P is the average daily precipitation in mm, and ET_0 is the potential daily evapotranspiration in mm. The Blaney-Criddle algorithm was used to

Fig. 1 Schematic overview of DECONIT. Boxes represent pools; arrows represent fluxes
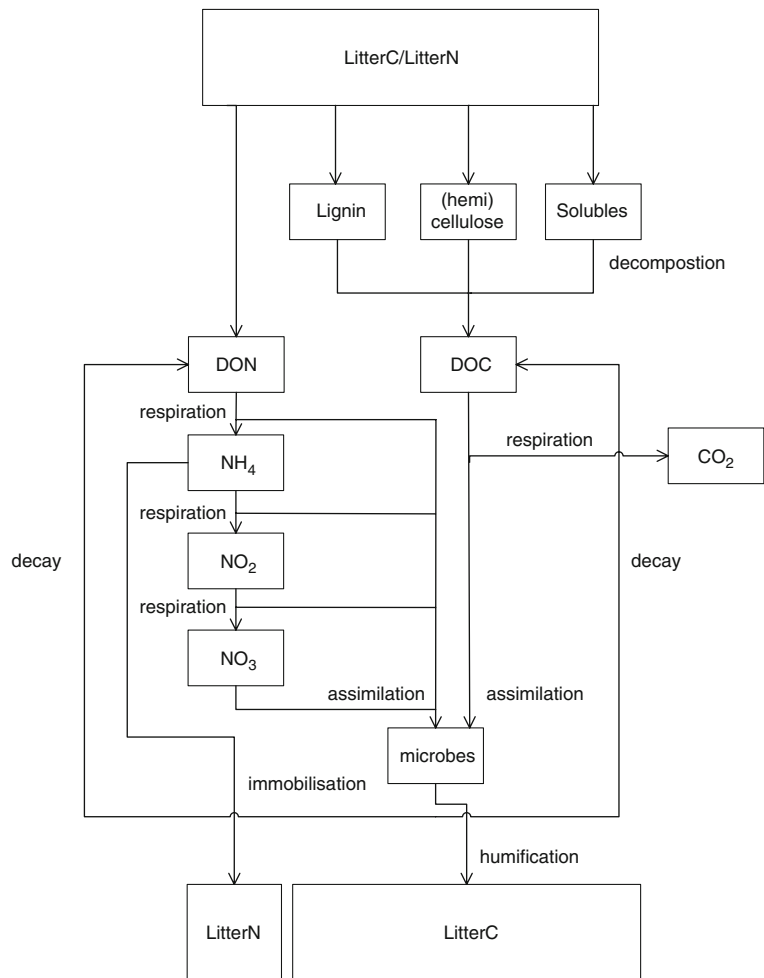
estimate ET_0. This approach was used, since ET_0 can be calculated with a restricted set of parameters (Blaney and Criddle 1950), since for many experiments only latitude, site temperature and precipitation are available.

Microbes can immediately digest smaller molecules, such as sugars, whereas larger molecular structures are typically fragmented by extra cellular enzymes before digestion (Roberts 1977). Although model approaches have been developed to study exoenzymatic activity, means to validate such approaches are limited (Schimel and Weintraub 2003). Therefore, DECONIT is still using a classic first-order decomposition approach. Thereby we acknowledge, that such an approach entails the assumptions, that exoenzymes are present immediately adjacent to the litters, and that decomposition delays for larger structures can be expressed implicitly in potential decomposition rates. We therefore equate DOC production directly to the carbon content of the disappearing litter, not considering any instantaneous CO_2 release for the breakdown of complex organic matter:

$$\left(\frac{\delta DOC}{\delta t}\right)_{dec} = \sum_{i=1}^{3} \frac{\delta L_i}{\delta t} \tag{7}$$

Mobilisation of DON is coupled to the decomposition of lignin according to:

$$\frac{\delta DON}{\delta t} = K_3 \cdot L_N \tag{8}$$

Besides decomposition also the description of the dynamic of microbial growth on different substrates is critical in biogeochemical models. Most models (e.g. DNDC) use a MM equation to relate microbial growth to substrate availability (Li et al. 1992). The use of MM implies that the population increment at lower substrate levels increases linearly with available substrate until it reaches a constant level μ_{max}, at which

Table 1 Notations variables

Variables	Description	Value	Min	Max	Unit	
L	Litter component	–	–	–	gC	
DOC	Dissolved organic carbon	–	–	–	gC	
DON	Dissolved organic nitrogen	–	–	–	gN	
NH_4^+	Ammonium pool	–	–	–	gN	
NO_2^-	Nitrite pool	–	–	–	gN	
NO_3^-	Nitrate pool	–	–	–	gN	
B	Microbial population size	–	–	–	gC	
HUMC	Humus pool (carbon content)	–	–	–	gC	
HUMN	Humus pool (nitrogen content)	–	–	–	gN	
f_{sub}	Substrate related growth reduction factor	–	–	–	–	
fn	Combined nitrogen substrate availability related growth reduction factor	–	–	–		
τ	Temperature correction factor	–	–	–	–	
CNL	ligninC/total nitrogen	–	–	–	$gCgN^{-1}$	
parameters						
$K_{SOLUTES}$	Potential decomposition rate of solutes	–	0	0.01	$gC\ gC^{-1}d^{-1}$	Uninformative
$K_{CELLULOSE}$	Potential decomposition rate of cellulose	–	0	0.01	$gC\ gC^{-1}d^{-1}$	Uninformative
K_{LIGNIN}	Potential decomposition rate of lignin	–	0	0.1	$gC\ gC^{-1}\ d^{-1}$	Uninformative
T_{OPT}	Optimum temperature for decomposition	–	10	50	°C	Coûteaux et al. (2002) Chen et al., (2000)
Q_{10}	Decomposition rate response to a 10°C warmer ambient temperature	–	2	5	$10°C^{-1}$	Davidson and Janssens, (2006)
$μ_{max}$	Potential microbial growth rate	–	0	5	$gC_{mic}\ gC_{mic}^{-1}d^{-1}$	Leffelaar & Wessel, (1988)
K_{DOC}	Half-optimum concentration of DOC for microbial assimilation	–	0	15	$mgCgDW^{-1}$	Leffelaar and Wessel, (1988)
K_{DON}	Half-optimum concentration of DON for microbial assimilation	–	0	15	$mgNgDW^{-1}$	Leffelaar and Wessel, (1988)
K_{NH4}	Half-optimum concentration of NH_4^+ for microbial assimilation	–	0	15	$mgNgDW^{-1}$	Leffelaar and Wessel, (1988)
K_{NO2}	Half-optimum concentration of NO_2^- for microbial assimilation	–	0	15	$mgNgDW^{-1}$	Leffelaar and Wessel, (1988)
K_{NO3}	Half-optimum concentration of NO_3^- for microbial assimilation	–	0	15	$mgNgDW^{-1}$	Leffelaar and Wessel, (1988)
Y_{DON}	Efficiency of DON assimilation	–	0	1	$gC_{mic}\ gN^{-1}$	Uninformative
Y_{NH4}	Efficiency of NH_4[a] assimilation	–	0	1	$gC_{mic}\ gN^{-1}$	Uninformative
Y_{NO2}	Efficiency of NO_2^- assimilation	–	0	1	$gC_{mic}\ gN^{-1}$	Uninformative
Y_{DOC}	Efficiency of DOC assimilation	–	0	1	$gC_{mic}\ gC^{-1}$	Uninformative
D	Microbial decay rate	–	0	1	$gC_{mic}gC_{mic}^{-1}d^{-1}$	Uninformative
F_{HUM}	Allocation of microbial detritus to humus	–	0	1	$gCgC^{-1}$	Uninformative
F_{IN}	Nitrogen immobilisation rate	–	0	1	$gNgN^{-1}d^{-1}$	Uninformative
Initials		–				
I_{LIGNIN}	Initial concentration of lignin[a]	–	300	600	$mg\ gDW^{-1}$	Berg et al. (1991a) Berg et al. (1991a)
I_{CELL}	Initial cellulose concentration[a]	–	300	600	$mg\ gDW^{-1}$	
I_{MB}	Initial concentration of microbial biomass	–	0	10	$mgC_{mic}\ gDW^{-1}$	Uninformative

Table 1 (continued)

Variables	Description	Value	Min	Max	Unit	
constants						
CNB	C:N ratio of microbial tissue	–	4	5	$gCgN^{-1}$	Frieder and Gabel., (2001)
F_H	Fraction of microbial detritus that humidifies	–	0	1	$gCgC^{-1}$	Uninformative
D	Fraction of microbial biomass per day lost by decay or respiration.	–	0	0.1	$gCgC^{-1}$	Uninformative
subscripts						
i	Litter types (cellulose, solutes, lignin)	–	–	–	–	
ass	Assimilation flux	–	–	–	–	
resp	Respiration flux	–	–	–	–	
decay	Detritus flux	–	–	–	–	
dec	Decomposition flux	–	–	–	–	
DOC	Dissolved organic carbon	–	–	–	–	
Parameter vectors						
$(pV)\overrightarrow{}_{new}$	Constructed parameter vector for a new run in the MCMC chain	–	–	–	–	
$(pV)\overrightarrow{}_{lastAccepted}$	Last accepted parameter vector in the MCMC chain	–	–	–	–	
ε	Parameter that determined the size of the parameter jump	–	–	–	–	
S	Random number between 0 and 1	–	–	–	–	

[a] Parameterised initials are only used when relevant datasets supplied no measured values

the microbes are unable to assimilate more substrate. In a nutrient-saturated environment, microbial growth rate is defined as an intrinsic characteristic of the population (Eq. 9 and 10)

$$\frac{\delta B}{B\delta t} = \mu_{max} \cdot f_s \qquad (9)$$

where $\frac{\delta B}{B\delta t}$ is the relative growth rate of microbial population B reduced by a factor f_s that is calculated from the availability of substrate S according to:

$$f_s = \frac{S}{K_S + S} \qquad (10)$$

where K_s is the substrate level at which the microbes obtain half their optimum growth rate. In the DECONIT model we further developed the outline approach by considering the effect of two growth-limiting substrates, i.e. carbon and multiple sources of nitrogen, on microbial growth. This is done by using a double MM equation (Shah and Coulman 1978), with f_N representing one growth reduction factor which depends on multiple nitrogen species (see also below):

$$\frac{\delta B}{B\delta t} = \mu_{max} \cdot f_{DOC} \cdot f_N \cdot B \qquad (11)$$

Such a formulation reduces to the normal MM equation when one of both substrates is in excess. The product of scaling factors f_{DOC} and f_N will result in generally more conservative estimates of the potential microbial growth rate than equation 1. This effect is to some extent compensated for by the alternative adjustment of the MM equation that is used in DECONIT to calculate f_N. The latter down regulates microbial growth as affected by the availability of four potential sources of nitrogen: DON, NH_4^+, NO_2^- and NO_3^-. This combined nitrogen availability factor is built reiteratively from combinations of two substrate factors. When microbial growth depends on two substrates, which can be considered to be facultative, the relationship between microbial growth and the levels of these two substrates is well described as:

$$\frac{\delta B}{B\delta t} = \mu_{max}(f_1 + f_2 - f_1 \cdot f_2) \qquad (12)$$

The effects of the two substrates on population growth are additive when both substrates are in minimal supply; the equation reduces to the MM equation when one substrate is depleted or to μ_{max}

when one or both substrates are in excess. Moreover, the effect of a nitrogen species, relevant to microbial assimilation, depends on the availability of the other nitrogen species, and the combined nitrogen response function is an asymptotic saturation curve similar to the individual nitrogen response curves. When applied to three substrates, substitution transforms the equation into:

$$\frac{\delta B}{B\delta t} = \mu_{max}f_3 + (f_1 + f_2 - f_1 \cdot f_2) - f_3(f_1 + f_2 - f_1 \cdot f_2) \quad (13)$$

where the effect of the substrates on population growth are additive when the substrates are in minimal supply. Eq. 13 reduces to Eq. 12 when one substrate is depleted, to the regular MM equation, when two substrates are depleted or to μ_{max} when any substrate is excessively available. Substitution is used again to include a fourth nitrogen species in DECONIT (i.e. DON, NH_4^+, NO_2^- and NO_3^-).

In DECONIT the fraction of the potential microbial growth rate that can be maintained with a given level of available DOC is calculated as:

$$f_{DOC} = \frac{DOC}{K_{DOC} + DOC} \quad (14)$$

Microbial biomass is expressed in terms of carbon. Consumption of DOC can therefore be calculated from microbial growth with a substrate specific loss factor (Y_{DOC}) for growth respiration:

$$\left(\frac{\delta DOC}{\delta t}\right)_{ass+resp} = \left(\frac{\delta B}{\delta t}\right)_{ass} / Y_{DOC} \quad (15)$$

CO_2 production complements carbon assimilation to account for the quantity of DOC that is consumed:

$$\frac{\delta CO_2}{\delta t} = \left(\frac{\delta B}{\delta t}\right)_{ass} \cdot (1.0/Y_{DOC} - 1.0) \quad (16)$$

Microbial nitrogen demand is derived from microbial growth and the microbial C:N ratio. Oxidation of the nitrogen species is calculated from assimilative nitrogen consumption and assimilation efficiency of the individual nitrogen species, equivalent to equation 16 (not shown). The contributions of the different

nitrogen elements to microbial growth are calculated by comparing the saturation levels of the individual nitrogen substrates with their sum:

$$\left(\frac{\delta DON}{\delta t}\right)_{ass+resp}$$
$$= \left(\frac{f_{DON}}{f_{DON} + f_{NH4} + f_{NO2} + f_{NO3}}\left(\frac{\delta B}{\delta t}\right)_{ass}\right) / CNB / Y_{DON} \quad (17)$$

$$\left(\frac{\delta NH_4}{\delta t}\right)_{ass+resp}$$
$$= \left(\frac{\delta DON}{\delta t}\right)_{resp} - \left(\frac{f_{NH4}}{f_{DON}+f_{NH4}+f_{NO2}+f_{NO3}}\left(\frac{\delta B}{\delta t}\right)_{ass}\right) / CNB / Y_{NH4} \quad (18)$$

$$\left(\frac{\delta NO_2}{\delta t}\right)_{ass+resp}$$
$$= \left(\frac{\delta NH_4}{\delta t}\right)_{resp} - \left(\frac{f_{NO2}}{f_{DON}+f_{NH4}+f_{NO2}+f_{NO3}}\left(\frac{\delta B}{\delta t}\right)_{ass}\right) / CNB / Y_{NO2} \quad (19)$$

$$\left(\frac{\delta NO_3}{\delta t}\right)_{ass} = \left(\frac{\delta NO_2}{\delta t}\right)_{resp} - \left(\frac{f_{NO3}}{f_{DON}+f_{NH4}+f_{NO2}+f_{NO3}}\left(\frac{\delta B}{\delta t}\right)_{ass}\right) / CNB \quad (20)$$

Where CNB is a constant microbial C:N ratio, the Y_x terms are substrate specific efficiency fractions and the f_x terms are substrate related growth correction factors. The saturation terms (f_{Nx}) are used to quantify relative contributions of the various nitrogen species as expressed in the quotients in equations 17–20 ($f_{Nx} / \sum_{i=1}^{4} f_{Nx}$ where $i=$DON, NH_4^+, NO_2^- and NO_3^+). These ensure that the microbes are flexible in their response to the substrates at their disposal. Continuous differentiability is maintained with low substrate levels because the contribution of each element to microbial growth proportionally decreases with its availability. Finally, the nitrogen balance is demonstrably closed since $\sum_{i=1}^{4}\left(f_{Nr} / \sum_{i=1}^{4} f_{Nx}\right) - 1.0$.

The COUP model (Jansson and Karlberg, 2004) and the PnET-N-DNDC model (Li et al 2000) relate the death rate of the microbial population (microbial decay) with microbial activity or the rate of assimilation. Such inclusions are generally motivated from laboratory findings that indicate how microbial growth responds with a certain delay, when environmental

conditions improve after a dire period (Blagodatsky and Richter, 1998). Even when such effects have been observed in the laboratory, however, it is unclear to what extent microbial dynamics in the field is affected. In DECONIT microbial decay was therefore implemented as a constant fraction of the population that is lost. This was done for reasons of parsimony and to maximise degrees-of-freedom. Similarly, in DECONIT maintenance respiration is understood as a constant fraction of the microbial population, allowing us to combine decay and maintenance to a single population size dependent parameter D.

$$\left(\frac{\delta B}{\delta t}\right)_{decay} = D \cdot B \qquad (21)$$

Carbon that converts to humus is quantified as a constant fraction of the microbial detritus flux:

$$\left(\frac{\delta HUMC}{\delta t}\right)_{decay} = F_H \cdot \left(\frac{\delta B}{\delta t}\right)_{decay} \qquad (22)$$

where F_H is the fraction of the microbial population that dies, and converts to the humus component. The humus is assumed stable, which is valid when simulating a relatively short period of a few years. In order to restrict the number of model parameters, the fraction of the microbial nitrogen compounds that accumulates in humus is assumed equal to the fraction of microbial carbon that accumulates. Additional nitrogen accumulates in humus when low molecular nitrogen (NH_4^+) reacts with degrading lignin to form humus compounds, which is in agreement with Berg (2000).

$$\left(\frac{\delta HUMN}{\delta t}\right)_{decay} = F_H \cdot \left(\frac{\delta B}{\delta t}\right)_{decay} \Big/ CNB + F_{IN} \cdot NH_4 \qquad (23)$$

In DECONIT carbon contents of microbial tissue that is not converted to humus, decays to DOC.

$$\left(\frac{\delta DOC}{\delta t}\right)_{decay} = (1.0 - F_H) \cdot \left(\frac{\delta B}{\delta t}\right)_{decay} \qquad (24)$$

Microbial nitrogen that dissolves during the decay of carcasses equals the nitrogen that is released from microbial detritus, subtracted with that which is humified.

$$\left(\frac{\delta DON}{\delta t}\right)_{decay} = \left(\frac{\delta B}{\delta t}\right)_{decay} \Big/ CNB - F_H \cdot \left(\frac{\delta B}{\delta t}\right)_{decay} \Big/ CNH \qquad (25)$$

DECONIT is integrated with time steps of one day.

Datasets

The data used in our study originate from 56 incubation experiments with 14 different plant species (Table 2). Unfortunately, however, concentrations of DON or NH_4^+ in such field incubation experiments will depend on a variety of interacting "uncontrolled" climatic factors. In order to have some insurance that measured concentrations were indeed related to the decomposition process, we used laboratory measurements to estimate parameters that are relevant for DON and NH_4^+ concentrations, microbial biomass and basal respiration. In sum, we used two types of datasets. 1) Field incubations on remaining organic litter substance, lignin, cellulose and nitrogen concentrations. Most data that is part of this dataset is published in Berg et al. (1991a) and Berg et al. (1991b). In order to add more datasets, some datasets were used that did not include all relevant tissues. Criterion to include poorer datasets was whether the dataset was of an underrepresented tissue (e.g. fine roots, Table 2, case 25) or species (e.g. Norway spruce, Table 2, cases 18–24). 2) Comprehensive datasets that were derived from laboratory incubations. Joanisse et al.(2008) measured remaining tissue dry weight, nitrogen concentrations, DON, NH_4^+, microbial biomass, and basal respiration in the laboratory, but unfortunately did not include measurements of lignin or cellulose concentrations.

An additional separation of the datasets into data that is used for model calibration and one that is used to evaluate the model on independent data is common. However, since decomposition rates measured under controlled laboratory conditions can not directly be compared with decomposition rates as measured under field conditions, and, thus, also model parameterisation will differ, we split our dataset in the four subsets C1, C2, E1 and E2 (Table 2). C generally refers to measurements that were used to calibrate the model, E to evaluate the model. The subscript one indicates field measurements and subscript two laboratory incubations.

Criteria for goodness-of-fit

The goodness-of-fit of the model was analysed using a framework for analysis of model performance proposed by Whitmore (1991). Consequently, we

Table 2 Datasets and references. [I] Status of the dataset in the development of the model (*C* Calibration or *E* Evaluation , 1= field incubations, 2=laboratory incubations) [II]Available measurements: RM refers to remaining litter organic substance (remaining matter, %DW), L: Lignin concentrations (mg gDW^{-1}), C: Cellulose concentrations (mg gDW^{-1}), N: Nitrogen concentrations (mgN gDW^{-1}). [III]Average annual site temperature and (in brackets) annual temperature spread. [IV]Initial nitrogen concentration of litter, [V]Initial lignin concentration of the litter

	S[I]	Species	Tissue	Measured[II]	T.[III]	IN[IV]	IL[V]	reference
1	C1	Barley	Stems	RM,L,C,N	5.4[10.75]	5.8	177	Wessén and Berg (1986)
2	C1	Myrtle	Leaves	RM,L,C,N	18.2[8.7]	12.9	179.8	Fioretto et al.(2005)
3	C1	Hairy rockrose	Leaves	RM,L,C,N	18.2[8.7]	19.4	335.2	Fioretto et al.(2005)
4	C1	Holm oak	Leaves	RM,L,C,N	18.2[8.7]	17.6	148.2	Fioretto et al.(2005)
5–14	C1	Scots pine	Needles	RM,L,C,N	3.8[10]	3.6–8.4	224–350	Berg et al.(1991a, 1991b)
15–17	C1	Scots pine	Needles	RM,L,N	8.7[9]	3	241	Berg et al.(1991a, 1991b)
18–24	C1	Norway spruce	Needles	RM,L,N	3.2[10]	4.2–18.3	242–431	Berg et al.(1991a, 1991b)
25	C1	Norway spruce	Fine roots	RM,N	5[10]	12.16	n.d.	Lohmus and Ivask (1995)
26	C1	Barley	Stems	RM,L,C,N	5.8[13.75]	5.9	61	Henriksen and Breland(1999)
27	C1	Ryegrass foliage	Leaves	RM,L,C,N	5.8[13.75]	18.1	14	Henriksen and Breland(1999)
28	C1	White cabbage	Leaves	RM,L,C,N	5.4[10.75]	15.9	7	Henriksen and Breland(1999)
29	C1	While clover	Leaves	RM,L,C,N	5.4[10.75]	41.5	2.9	Henriksen and Breland(1999)
30	C1	Potato	Stems	RM,L,C,N	5.8[13.75]	26	65	Henriksen and Breland(1999)
31–45	E1	Scots pine	Needles	RM,L,N	1.3[10.75]	3.0–13.4	229–381	Berg et al.(1991a, 1991b)
46–50	E1	Lodgepole pine	Needles	RM,L,N	3.8[10]	3.4–4.1	257–389	Berg et al.(1991a, 1991b)
51	C2	Black spruce and Sheep laurel	Needles / Leaves	RM,N,DON,NH4, MB,BR	20[0]	6	n.d.	Joanisse, et al.(2008)
52–56	E2	Black spruce and Sheep laurel	Needles / Leaves	RM,N,DON,NH4, MB,BR	20[0]	6	n.d.	Joanisse, et al.(2008)

present coefficients of determination (R^2), mean modelled and mean measured values, and F-ratios.

Model calibration

A Markov Chain Monte Carlo approach was used to calibrate the model. Since this method has been described in detail by other authors (Metropolis et al. 1953; Braswell et al. 2005; Zobith et al. 2008), we limit our discussion to the general concept and mention settings that are typical for this study.

The model is run iteratively (100,000 times for each dataset) with parameters that are constructed according to:

$$(pV)_{new}^{\rightarrow} = (pV)_{lastAccepted}^{\rightarrow} + s \cdot (\varepsilon)^{\rightarrow} \left((pV)_{max}^{\rightarrow} - (pV)_{min}^{\rightarrow} \right) \tag{26}$$

Where $(pV)_{new}^{\rightarrow}$ is the parameter vector that is used to define the model in the relevant chain position. The parameter uncertainty range $(pV)_{max}^{\rightarrow} - (pV)_{min}^{\rightarrow}$ is defined a-priori for a given parameter. We assumed that the a-priori parameter probabilities are uniform

over a wide range. Candidate parameter vectors $(pV)_{new}^{->}$ are constructed from the last accepted parameter vector $(pV)_{lastAccepted}^{->}$ that is defined by the ratio (α) of previous and current natural logarithm of the model likelihood (L) when it exceeds a random number between 0.0 and 1.0. When the model fit has improved, α exceeds 1.0 and the running parameter vector $(pV)_{new}^{->}$ is passed to $(pV)_{lastAccepted}^{->}$. When the model fit did not improve, $(pV)_{new}^{->}$ is accepted with a rate equal to the difference in the natural logarithmic of L. This chance factor is used to allow the model to escape from local optima during its chain walk. Step size s is a random number that expresses the fraction of the a-priori parameter uncertainty range that is covered when ε, a random number that is normally distributed between -3 and 3 standard deviations, returns 1.0. It lacks a statistical meaning, but determines the efficiency with which a chain walk proceeds: large step sizes will potentially allow a fast exploration of parameter space; if not parameter vectors are frequently rejected. Using small step sizes, on the other hand, slows down the exploration of parameter space (Braswell et al. 2005). We found reasonable results when ε was set to 0.1. Assuming that all errors are Gaussian distributed, we can calculate model likelihood L from the pairs of measured and modelled values according to:

$$L = \prod_{i=1}^{n} \frac{1}{\sqrt{2\pi}\sigma_n} e\left(\frac{x_i - \eta_i}{2\sigma_n^2}\right) \qquad (27)$$

When measurement types differ, as in this study (remaining tissue dry weight and lignin, cellulose, nitrogen concentrations), the standard deviation σ_n^2 defines how the different objectives are weighted to calculate L. In cases where replicates were unavailable, we generally assumed 10% measurement uncertainty. The calibration keeps track of the parameter vector associated with the maximum posterior likelihood (MAP=maximum a-posterior probability).

None of the model parameters is known with great precision and moreover, parameters can be slightly differently defined in various models, e.g. in our model, a "K" value does not mean the same as when conceptually defined decomposition pools are used. In order not to restrict parameter estimations too much by previous published finding, we have generally used upper and lower values that were published as our a-priori ranges (Table 1).

Parameter sensitivity

Marginal probability distributions, e.g. plots of parameter values with the number and values of parameter vectors that were accepted in the chain, can be derived from parameter vectors that were included in the MCMC. The shapes of posterior probability distributions give an impression of the model sensitivity for a particular parameter. The coefficient of variation (=standard deviation of accepted parameter values/mean accepted parameter value) can be used to express model sensitivity for a parameter, i.e. small values denote sensitive model parameters (Van Oijen et al. 2005). We used the standard deviation of the parameter estimates of the sites as a measure to indicate posterior parameter uncertainties.

Results

Estimates for decomposition rates in a field situation

Results of model applications are shown in Fig. 2. The model successfully mimicked remaining litter organic substance (C1 datasets), with coefficients of determination ranging from R^2=0.72 (n=10) for Scots pine needles (Tables 2, 3 and 4: case 10) to R^2=0.95–1.00 for 20 out of 30 cases (with n being the temporal replication ranging from 3 to 15). Predictions of remaining litter organic substance (evaluation dataset E1; Table 2: cases 31–49) were similarly successful. We found coefficients of determination ranging from R^2 = 0.87 (n=4) for Scots pine needles (Table 2, 4: case 45) to R^2 ranging from 0.90 to 1.00 for 18 out of 19 cases (n ranging from 4 to 12). In general, model agreement with measured concentrations of lignin was somewhat lower. Coefficients of determination for the calibration dataset C1 (Table 2) ranged from R^2=0.11 (n=11) for Hairy rockrose to R^2=0.90–0.99 (n ranging between 3 and 15) for 12 out of 24 cases. For the evaluation dataset E1 (Table 2), we found coefficients of determination ranging from R^2 = 0.87 for Scots pine needles (Table 2, 4: case 45) to R^2 = 0.95–1.00 for 11 out of 19 experiments (n ranging from 4 to 12). Model agreement with measured concentrations of cellulose (e.g. the C1 dataset) in decomposing litters was typically lower. Coefficients of determination were ranging from R^2 = 0.01 for
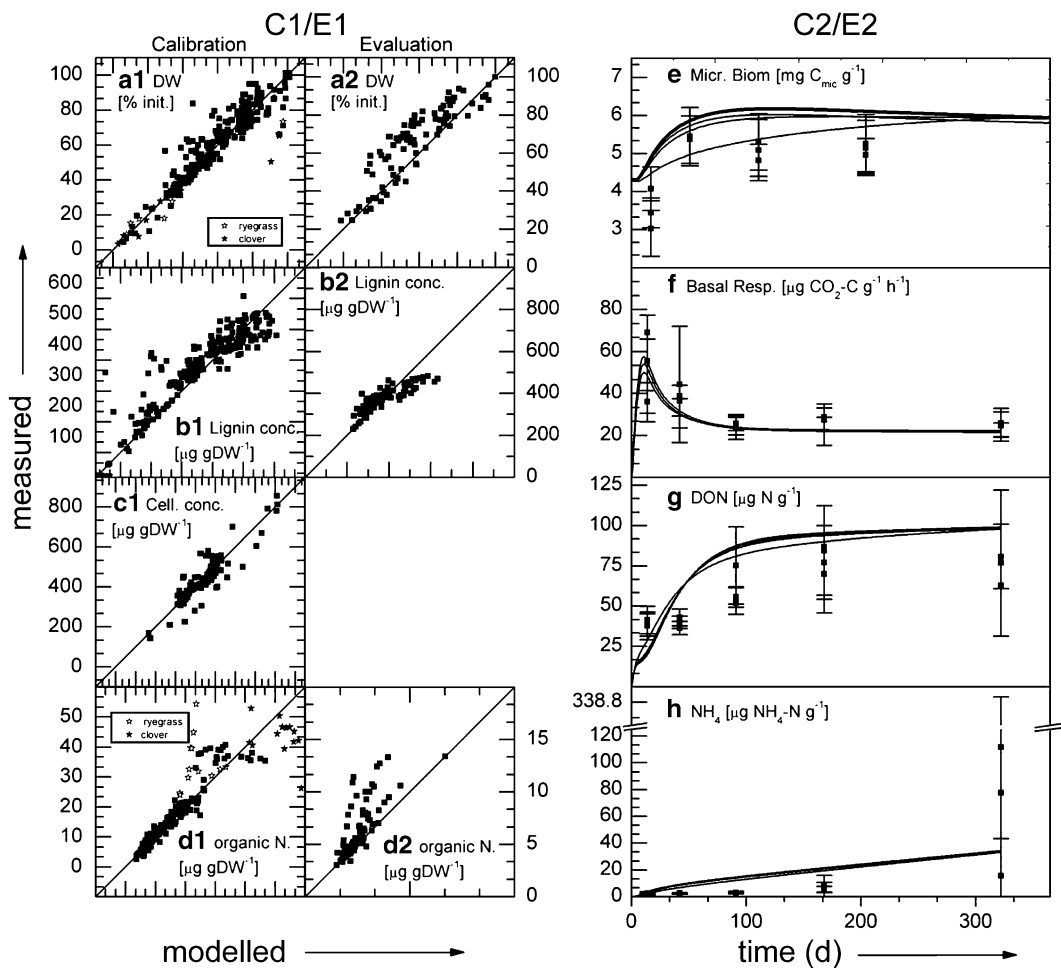
Fig. 2 Modelled and measured concentrations of different tissue structures: **a** Remaining tissue dry weight, **b** lignin concentrations, **c** cellulose concentrations, **d** nitrogen concentrations. The left panel with graphics e-h show measured and simulated temporal dynamics of microbial biomass, **f** basal respiration **g** concentrations of DON and h) concentrations of NH_4^+. C1/E1 and C2/E2 indicates the calibration and the evaluation datasets

Scots pine needles (Table 2, 4: case 6, $n=4$) to $R^2=$ 0.60–0.78 for 5 out of 19 experiments. The model generally agreed well with measured nitrogen concentrations. Holm oak leaves (Table 2, 4: case 4, $n=$ 11) were exceptional since the model agreement was low, with a coefficient of determination of $R^2=0.03$ ($n=11$). In general, coefficients of determination were ranging from $R^2=0.70$ to $R^2=1.00$ for 23 out of 30 cases. For the evaluation dataset for field incubations E1, we found coefficients of determination ranging from $R^2=0.6$ for Scots pine needles (Table 2, 4: case 44, $n=4$) to 0.9–1.0 for 9 out of 16 sites.

The DECONIT model did not work for all cases, e.g. nitrogen concentrations in Holm oak leaves (Table 2, 4: case 4), lignin concentrations in Hairy rockrose

(Table 2, 4: case 3) or litter organic substance in a sample of Scots pine needles were not well captured (Table 2, 4: case 10).

In the case Holm oak leaves (Table 2, 4: case 4, $R^2=$ 0.03, $n=11$) we dealt with leaves that are relatively rich in nitrogen (17.6 gN gDW^{-1}). The F-ratio that is associated with modelled nitrogen concentrations is 2.3 ($p>0.1$). Hence model uncertainty is markedly larger than measurement uncertainty. In this particular experiment, a decomposition of lignin was not observed and moreover, nitrogen was strongly immobilised, e.g. only 10% had disappeared after two years of incubation (Fioretto et al. 2005). Moreover, since the initial concentration of nitrogen in the leaves was particularly high, observed delay of decomposition cannot be

Table 3 Parameter estimates (*MAP* maximum a-posterior probability, *CV* Coefficient of variation) for the potential decomposition rates (K_i), the temperature response parameters (Q_{10} and T_{OPT}), microbial growth (μMAX), half optimum concentrations (K_x), substrate use efficiencies (Y_z), allocation to the humus pool (F_{HUM}), immobilization of nitrogen (F_{IN}) and mean estimated initial concentrations of lignin, cellulose and solubles (if not measured) for the combined field (MAP^{C1}) and laboratory (MAP^{C2}) experiments. Dummy is a variable that was added to the parameters and given a range from 0.0 to 1.0. Dummy is not used in the model, hence its CV is a reference for a completely non-sensitive parameter. For units of parameters see Table 1

	C1			E1		
	MAP^{C1}	95% uncertainty range	CV^{C1}	MAP^{C2}	95% uncertainty range	CV^{C2}
K_{LIGNIN}	0.003	0.002	0.31	0.00034	0.003	0.6
K_{CELL}	0.006	0.004	0.49	0.00044	0.007	0.5
K_{SOL}	0.029	0.052	0.69	0.15016	0.075	0.6
Q_{10}	3.2	0.6	0.24	3.61	0.5	0.2
T_{OPT}	28.1	2.2	0.09	30.18	2.4	0.5
μ_{MAX}	2.4	1.1	1.48	1.97	1.2	0.2
K_{DOC}	10.6	5.3	1.76	7.77	4.3	0.5
K_{DON}	5.7	4.8	1.34	15.0	3.7	0.4
K_{NH4}	8.6	4.9	1.62	0.01	2.5	0..5
K_{NO2}	6.3	6.1	1.34	8.21	5.7	0.5
K_{NO3}	5.2	4.2	1.52	8.43	4.8	0.4
Y_{DON}	0.9	1.5	1.53	0.99	0.01	0.5
Y_{NH4}	0.5	1.4	1.69	0.53	0.6	0.5
Y_{NO2}	0.0	1.9	1.52	0.48	0.6	0.5
Y_{DOC}	0.5	1.1	1.69	0.48	0.5	0.6
D	0.06	0.2	0.06	0.06	0.02	0.2
F_{HUM}	0.01	0.5	1.67	0.56	0.5	0.5
F_{IN}	0.68	0.3	1.63	0.58	0.2	0.4
CNB	7.9	2.9	1.85	12.00	3.2	0.5
DUMMY[I]	0.51	0.45	1.67	0.51	0.4	1.5

explained well by nitrogen shortages of decomposing microbial communities. Neither the initial concentration of lignin, which is below average (148.2 g gDW^{-1}), nor the initial concentration of nitrogen can be used to explain this resistance to decomposition. For other cases, the DECONIT model was well predicting decomposition, even though litter was nitrogen richer as compared to litter derived from Holm oak leaves. Therefore, we assumed that some other factor was delaying the rate of decomposition. E.g. the incubation terrain may be of importance since the topography is a coastal area characterised by alluvial deposit dunes (Fioretto et al. 2005) and may support only low concentrations of decomposing microbial communities. Another case where the model failed to predict observed dynamics in decomposition, was in the case of Hairy rockrose or Myrtle leaves (Table 2, 4: case 3, $R^2=0.11$, $n=11$ and case 2, $R^2=0.21$, $n=11$). For both litter types the lignin component was decomposing much slower than would be expected from other datasets. All of these incubations took place in Southern Italy. Possible explanations are again the location of this particular site (Fioretto et al. 2005). Alternatively, the decomposition of recalcitrant materials may be more sensitive to temperature or moisture conditions than the decomposition of the other components.

Microbial biomass, DON, NH_4^+ and basal respiration in laboratory experiments

Predictions by DECONIT were in general in good agreement with observed microbial biomass dynamics (Table 2, 4: cases 51–56). For the calibration dataset, the coefficient of determination was $R^2=0.86$ and for the evaluation datasets (Table 2, 4: cases 52–56), we

Table 4 Criterion for the goodness-of-fit of remaining litter dry weight, lignin concentration, cellulose concentration, organic nitrogen content, DON, NH_4^+, microbial biomass (MB) and basal respiration (BR) for all the datasets used for this contribution. Used abbreviations m number of measurements, n number of repetitions, F the F-test criterion

site	Remaining litter [% initial]					Lignin conc [mg gDW⁻¹]					Cellulose conc [mg gDW⁻¹]					organic nitrogen conc [mgN gDW⁻¹]					DON conc [μgN gDW⁻¹]					NH4⁺ conc [μgN gDW⁻¹]					MB [mg gDW⁻¹]					BR [μg CO2-C gDW⁻¹ h⁻¹]				
	m	n	M	F	R²	m	n	M	F	R²	m	n	M	F	R²	m	n	M	F	R²	m	n	M	F	R²	m	n	M	F	R²	m	n	M	F	R²	m	n	M	F	R²
1	15	42	8.7	0.4	0.85	15	42	24	2	0.55	9	24	26	6	0.06	15	42	1.7	0.1	0.75	0	0				0	0				0	0				0	0			
2	11	100	7.1	3.4	0.92	11	100	63	12	0.21	11	100	64	21	0.60	11	100	1.3	0.2	0.79	0	0				0	0				0	0				0	0			
3	11	100	3.3	0.4	0.97	11	100	66	4	0.11	11	100	74	3	0.06	11	100	1.6	0.7	0.79	0	0				0	0				0	0				0	0			
4	10	90	4.3	1.6	0.96	10	90	87	5	0.12	10	90	25	16	0.13	10	90	2.3	2.3	0.03	0	0				0	0				0	0				0	0			
5	4	60	5.1	3.2	0.89	4	60	4	3	0.96	4	60	26	22	0.08	4	60	0.8	0.7	0.78	0	0				0	0				0	0				0	0			
6	4	60	3.5	2.3	0.94	4	60	8	1	0.98	4	60	25	34	0.01	4	60	0.6	0.4	0.83	0	0				0	0				0	0				0	0			
7	4	60	3.4	2.6	0.95	4	60	9	5	0.98	4	60	11	36	0.05	4	60	0.4	0.4	0.86	0	0				0	0				0	0				0	0			
8	4	60	2.1	1.4	0.97	4	60	48	12	0.18	4	60	14	12	0.27	4	60	0.7	2.3	0.77	0	0				0	0				0	0				0	0			
9	10	180	2.6	2.7	0.98	9	160	27	7	0.94	9	160	14	21	0.63	10	180	0.5	0.1	0.93	0	0				0	0				0	0				0	0			
10	10	180	6.1	5.1	0.72	10	180	34	10	0.96	10	180	20	13	0.78	10	180	0.9	0.1	0.97	0	0				0	0				0	0				0	0			
11	10	180	1.6	1.3	0.99	10	180	34	7	0.93	10	180	17	12	0.72	10	180	0.9	0.1	0.97	0	0				0	0				0	0				0	0			
12	10	180	2.1	1.2	0.99	10	180	35	8	0.93	10	180	15	14	0.59	10	180	0.7	0.3	0.91	0	0				0	0				0	0				0	0			
13	10	180	2.7	0.8	0.98	10	180	45	9	0.89	10	180	18	17	0.55	10	180	1	0.3	0.84	0	0				0	0				0	0				0	0			
14	6	100	3.4	4	0.98	6	100	42	6	0.97	6	100	16	21	0.63	6	100	0.3	0.1	0.98	0	0				0	0				0	0				0	0			
15	6	116	10.1	1.5	0.88	6	116	21	8	0.96	0	0				6	116	1.7	2.7	0.93	0	0				0	0				0	0				0	0			
16	5	98	8.2	0.5	0.93	4	71	10	4	0.99	0	0				4	71	1.5	1.6	1	0	0				0	0				0	0				0	0			
17	4	75	6.7	0.5	0.92	3	50	12	6	0.99	0	0				3	50	0.9	0.8	0.99	0	0				0	0				0	0				0	0			
18	11	334	3	0.1	0.95	11	334	36	1	0.77	0	0				11	334	0.9	0.4	0.94	0	0				0	0				0	0				0	0			
19	11	235	6.7	0.7	0.84	11	235	45	6	0.76	0	0				11	235	0.8	0.1	0.96	0	0				0	0				0	0				0	0			
20	12	287	2.4	0.2	0.96	12	287	21	0	0.51	0	0				5	147	0.6	0.2	0.7	0	0				0	0				0	0				0	0			
21	14	391	3.9	0.3	0.88	14	391	13	0	0.94	0	0				4	146	0.6	0.4	0.98	0	0				0	0				0	0				0	0			
22	14	377	2.3	0.1	0.97	14	377	33	1	0.63	0	0				4	148	0.3	0.05	0.92	0	0				0	0				0	0				0	0			
23	6	196	6.6	2	0.94	6	196	41	14	0.89	0	0				4	146	1.3	1.20	0.99	0	0				0	0				0	0				0	0			
24	12	337	1.9	0.1	0.97	12	337	30	1	0.77	0	0				5	171	0.6	0.10	0.86	0	0				0	0				0	0				0	0			
25	13	36	4.6	0	0.85	0	0				0	0				12	33	0.4	0.1	0.85	0	0				0	0				0	0				0	0			
26	13	36	5.1	0.2	0.93	0	0				7	18	42	6	0.04	13	36	1.9	0.1	0.88	0	0				0	0				0	0				0	0			
27	13	36	7.1	0.7	0.89	0	0				7	18	138	33	0.01	13	36	9.4	15.5	0.1	0	0				0	0				0	0				0	0			
28	13	36	7.6	2.2	0.86	0	0				7	18	147	51	0.28	13	36	7.8	10.4	0.42	0	0				0	0				0	0				0	0			
29	13	36	8.9	1.2	0.9	0	0				7	18	156	23	0.27	13	36	7.3	39.3	0.27	0	0				0	0				0	0				0	0			
30	13	36	7	1.4	0.89	0	0				7	18	92	27	0.16	13	36	4.3	20	0.42	0	0				0	0				0	0				0	0			
31	5	93	4.8	0.8	0.99	5	93	28	5	0.99	0	0				4	76	0.8	0.5	0.9	0	0				0	0				0	0				0	0			
32	4	45	0.9	0	1	4	45	56	16	1.00	0	0				4	45	0.8	0.2	0.99	0	0				0	0				0	0				0	0			
33	4	45	0.9	0	1	4	45	56	16	1.00	0	0				4	45	0.8	0.2	0.99	0	0				0	0				0	0				0	0			
34	5	96	7.8	2.5	0.97	4	74	44	19	0.97	0	0				0	0				0	0				0	0				0	0				0	0			
35	5	98	1.9	0.2	1	5	98	34	9	1.00	0	0				2	25	1.1	1.6	1	0	0				0	0				0	0				0	0			

Table 4 (continued)

#	Remaining litter [% initial]					Lignin conc [mg gDW⁻¹]					Cellulose conc. [mg gDW⁻¹]	organic nitrogen conc. [mgN gDW⁻¹]					DON conc. [μgN gDW⁻¹]					NH₄⁺ conc. [μgN gDW⁻¹]					MB [mg gDW⁻¹]					BR [μg CO2-C gDW-1 h-1]				
36	5	95	1.5	0.1	0.99	0	0	0	0	0.99	0	0	0	0			0	0	0	0	0	0	0	0	0	0	0	0	0	0	0	0	0	0	0	0
37	5	99	2.1	0.2	0.99	4	75	35	13	0.99	0	0	0	0			0	0	0	0	0	0	0	0	0	0	0	0	0	0	0	0	0	0	0	0
38	5	100	2.2	0.3	0.95	5	100	38	19	0.95	0	5	100	0.2	0.1	0.85	0	0	0	0	0	0	0	0	0	0	0	0	0	0	0	0	0	0	0	0
39	7	148	4.4	0.8	0.94	7	148	51	24	0.94	0	5	99	1	0.6	0.97	0	0	0	0	0	0	0	0	0	0	0	0	0	0	0	0	0	0	0	0
40	5	99	3.1	0.6	0.93	5	99	37	15	0.93	0	5	99	0.5	0.2	0.95	0	0	0	0	0	0	0	0	0	0	0	0	0	0	0	0	0	0	0	0
41	7	145	3.3	0.4	0.95	7	145	14	2	0.95	0	7	145	0.5	0.2	0.97	0	0	0	0	0	0	0	0	0	0	0	0	0	0	0	0	0	0	0	0
42	7	148	4.3	0.7	0.94	6	125	18	3	0.94	0	6	125	0.4	0.1	0.86	0	0	0	0	0	0	0	0	0	0	0	0	0	0	0	0	0	0	0	0
43	7	148	4.3	0.7	0.93	5	98	13	2	0.93	0	5	98	0.2	0.1	0.87	0	0	0	0	0	0	0	0	0	0	0	0	0	0	0	0	0	0	0	0
44	5	98	2.2	0.4	0.92	4	75	60	89	0.92	0	4	75	0.9	1.5	0.6	0	0	0	0	0	0	0	0	0	0	0	0	0	0	0	0	0	0	0	0
45	4	73	3.5	0.6	0.87	3	49	52	57	0.87	0	3	49	0.9	1.5	0.78	0	0	0	0	0	0	0	0	0	0	0	0	0	0	0	0	0	0	0	0
46	11	221	21.1	6.6	0.94	11	221	34	3	0.94	0	11	221	3.5	4	0.79	0	0	0	0	0	0	0	0	0	0	0	0	0	0	0	0	0	0	0	0
47	5	95	11.9	4	0.99	5	95	71	23	0.99	0	5	95	1.2	0.8	0.93	0	0	0	0	0	0	0	0	0	0	0	0	0	0	0	0	0	0	0	0
48	12	252	18.9	8.1	0.98	12	252	16	1	0.98	0	12	252	2.2	1.8	0.94	0	0	0	0	0	0	0	0	0	0	0	0	0	0	0	0	0	0	0	0
49	11	237	20.9	8.6	0.94	11	237	36	6	0.94	0	11	237	3.8	4.8	0.78	0	0	0	0	0	0	0	0	0	0	0	0	0	0	0	0	0	0	0	0
50	5	94	10.5	2.8	0.98	5	94	56	12	0.98	0	5	94	0.6	0.3	0.74	0	0	0	0	0	0	0	0	0	0	0	0	0	0	0	0	0	0	0	0
51	6	30	1.4	0.03	0.83	0	0				0	5	24	1.5	0.31	0.66	5	24	0.01	0.04	0.90	5	24	0.02	0.00	0.67	5	24	0.9	0.07	0.85	5	24	5.8	1.09	0.92
52	6	36	1.8	0.02	0.73	0	0				0	5	30	1.5	0.19	0.00	5	30	0.01	0.02	0.76	4	24	0.01	0.00	0.85	4	24	0.9	0.04	0.89	5	30	4.9	0.51	0.58
53	6	30	0.8	0.01	0.95	0	0				0	5	24	1.5	0.23	0.08	5	24	0.02	0.08	0.73	5	24	0.02	0.00	0.72	5	24	0.7	0.04	0.49	5	24	4.2	0.30	0.91
54	6	30	1.5	0.03	0.72	0	0				0	5	24	1.5	0.24	0.18	5	24	0.02	0.31	0.71	5	24	0.02	0.00	0.84	5	24	0.9	0.04	0.83	5	24	6.6	0.85	0.92
55	6	30	1.5	0.02	0.74	0	0				0	5	24	1.5	0.16	0.20	5	24	0.02	0.03	0.72	5	24	0.02	0.00	0.66	5	24	0.9	0.03	0.87	5	24	6.9	0.34	0.99
56	6	30	1.7	0.03	0.81	0	0				0	5	24	1.5	0.31	0.66	5	24	0.01	0.00	0.91	5	24	0.03	0.01	0.57	5	24	0.7	0.04	0.86	5	24	6.9	2.07	0.81

found coefficients of determination ranging from $R^2 = 0.49$–0.89. In spite of these somewhat lower coefficients of determination, the model agreement was highly significant ($p<0.01$) in all cases because measurement uncertainty was considerable (Fig. 2e, Table 4).

For most litter types, microbial population size obtains a sigmoid shape, either or not followed by some loss of microbial biomass in a later stage (Fig 2e). The initial delay in simulated microbial growth is due to the initial microbial population size, which was assumed to be <5 mg microbial biomass C g^{-1} dry weight litter mass. At the beginning of the simulations microbial biomass growth is relatively slow due to nitrogen shortage. Related to the initial nitrogen limitation on microbial growth, is an accumulation of DOC in the initial phase of decomposition (not shown).

Coefficients of determination associated with the model performance on microbial respiration was $R^2 = 0.92$ for the calibration dataset C2 (e.g. Table 2, 4: case 51), and ranged from $R^2 = 0.58$ to $R^2 = 0.91$ for the evaluation datasets (Table 2, 4: case 52 to 56). Microbial respiration was typically high shortly after the start of incubation and decreased after an initial peak rate of approximately 53 µg CO$_2$–C g^{-1}h^{-1} to remain constant at around 20 µg CO$_2$-C g^{-1}h^{-1}. The model agreement with regard to measurements of microbial respiration was highly significant ($p<0.01$) for all experiments.

The model agreed well with measurements of concentrations of DON and NH$_4^+$ (Table 2 and 4: cases 51–56). Coefficients of determination were ranging from $R^2 = 0.70$–0.89 for DON ($p<0.01$ in all cases) and $R^2 = 0.54$ –0.85 ($p<0.01$) for model agreement with measured concentrations of NH$_4^+$. Measured concentrations of organic nitrogen typically increased faster in the first three months after the incubation, to stabilize in a later stage. Concentrations of NH$_4^+$ increased steadily throughout the incubation period.

Probability distributions and sensitivity analyses

Mineralization rate estimates differed markedly for the C1 (field) and the C2 (laboratory) dataset (Table 3). The gradient of decomposability corresponds with that which would be expected, e.g. K$_{LIGNIN}$<K$_{CELL}$<K$_{SOL}$ in both cases. An example

of a posterior likelihood distribution for a particularly sensitive model parameter, the optimal decomposition temperature (T$_{OPT}$), is shown in Fig. 3.

For many of the parameters on microbial dynamics e.g. K$_{(substrate)}$ or Y$_{(substrate)}$ values, the estimates were highly uncertain, which is reflected by large coefficients of variation (CV) and uncertainty intervals. The effectivity of ammonium consumption (e.g. Y$_{DON}$ or the fraction of DON, used by the microbes that is effectively converted to microbial tissue compared with that which is converted to NH$_4^+$) is a very sensitive model parameter given the data. For the laboratory experiments, values of Y$_{DON}$ indicate that the rate of microbial assimilation of DON exceeded the rate of ammonification.

Discussion

Comparison of model parameter estimates with published values

The estimated decomposition rates for the DECONIT model for lignin ($k=0.003\pm0.002$ d^{-1}) and cellulose (0.006 ± 0.004 d^{-1}) are similar to the optimum decomposition rates that are used for structural pools of decomposition tissue in DAYCENT ($k=0.0005 - 0.003$ d^{-1}, Wang et al., 2002). Also, the estimated
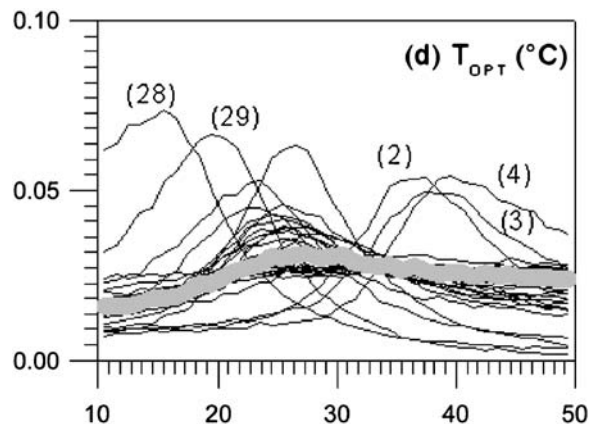
Fig. 3 Posterior (normalized) marginal probability distribution for the optimum temperature for decomposition (T$_{OPT}$). The thin black lines represent model likelihood as a function of model parameter values for the individual cases. The thick grey line represents the general probability distributions for all cases and litter types. The outliers are marked with numbers that correspond to the numbering of the cases in Table 2

decomposition rate of solutes (0.0286±0.052 d^{-1}) in DECONIT is similar to that of the disintegration rate of metabolic carbon in DAYCENT (0.003 – 0.03 d^{-1}, Wang et al. 2002). Kirschbaum (1995) reported that Q_{10} values ranged between 2.5 to 8.0 between different reports, but state that Q_{10} decreases with temperature. For comparison, we have found values from 2.0 to 3.99, when estimating Q_{10} values for individual sites (data not shown). The optimum value for all sites was Q_{10}=3.2±0.6. Mentioned papers that discuss the importance of Q_{10}, moreover, ignore the importance of the optimum temperature T_{OPT} for decomposition. We estimated that the optimum temperature for decomposition was 28.1±2.3°C. In comparison, Coûteaux et al (2002) used 25°C according to Lohmander et al. (1998). Chen et al (2000) found that decomposition may increase up to temperatures to 30°C–40°C, i.e. somewhat higher than 27°C, which was proposed by Braakhekke and De Bruijn (2006).

Carbon quality as a predictor of litter decomposability

Berg et al. (1993) found that actual evapotranspiration best explained variations in measurements of remaining tissues and organic matter (R^2_{adj} = 0.509). This conclusion was based on an extensive dataset, part of which was also used in this study (Berg et al 1991a; Berg et al 1991b). By comparison, we found R^2_{adj} = 0.46 for remaining organic matter, R^2_{adj} = 0.52 for remaining lignin, R^2_{adj} = 0.10 for cellulose and R^2_{adj} = 0.76 for nitrogen for the C1 datasets. Even though we used a very simple scheme for calculating moisture effects on decomposition, we found a similar goodness of fit as Berg et al. (1993) did. Furthermore, our results indicate that carbon quality ranks similar to climatic conditions to explain decomposition rates. We find support for such conclusion from a high-profile study that recently showed that differences in plant species litter traits are a better predictor to explain differences in decomposition rates rather than climatic conditions (Cornwell et al. 2008). The authors of this study suggest that most climax vegetation types are characterised by high nitrogen use efficiencies and are producing litter with high lignin contents. In other words this can be interpreted in such a way that litter properties are overriding effects of climate on decomposition.

Model applicability is low for initial lignin concentrations <180 mg gDW^{-1}

The model underestimated mineralization rates of lignin and nitrogen in decomposing leaves of Myrtle and Hairy rockrose (Table 3: case 2 and 3; initial nitrogen concentration 12.9 mgN gDW^{-1}, resp. 19.4 mgN gDW^{-1} initial lignin concentration 179.8 mg gDW^{-1} resp. 335.2 mg gDW^{-1}). Similarly, the model underestimated litter organic substance decomposition rates of ryegrass, clover leaves, cabbage leaves and potato stems, even though DECONIT is more accurate while estimating nitrogen concentrations in ryegrass and potato stems (Table 2: case 27–30).

An issue worth considering is whether these cases have in common a high initial concentration of nitrogen more often than a low initial concentration of lignin. Our findings applying the model to observations of decomposing leaves of the Hairy rockrose suggest that the model lacks performance for nitrogen rich litters. Myrtle leaves, ryegrass, clover leaves, cabbage leaves and potato stems however, are initially both nitrogen rich and lignin poor.

That low lignin concentrations rather than high nitrogen concentrations may be the reason for problems associated with predicting decomposition kinetics with DECONIT is illustrated by the following three cases. Barley straw is relatively poor in nitrogen and lignin (Table 2: case 1; initial nitrogen concentration 5.8 mg Ng DW^{-1} initial lignin concentration 177 mg gDW^{-1}) and the model failed to capture the loss of nitrogen during the first 200 days after the incubation (Fig. 4c). On the other hand, DECONIT was well able to predict the decomposition of nitrogen and lignin rich litters. Decomposition dynamics of needles of Norway spruce (Table 2: case 22 and case 24) having a high initial concentration of nitrogen (13.6 gN gDW^{-1} and 18.3 gN gDW^{-1}) and a high initial concentration of lignin (340 mg gDW^{-1} and 370 mg gDW^{-1}) was well predicted with regard to remaining litter organic substance or nitrogen concentrations.

Hence only one experiment (with leaves of the Hairy rockrose) indicates that the model underestimates decomposition rates for nitrogen rich litters, but two incubation experiments with pine needles or with barley straw conflict with such argument. Low initial concentrations of lignin, however, seem to be a more serious problem for the model, since the lack of
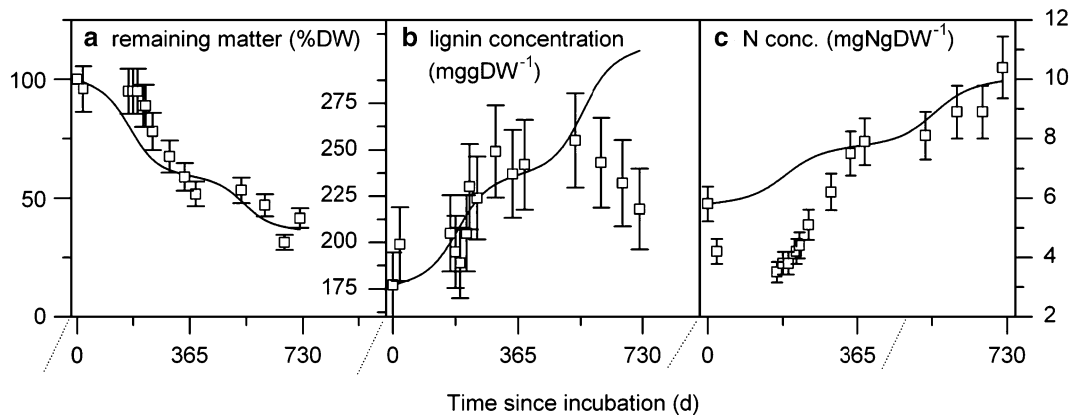
Fig. 4 Simulated and measured decomposition of barley straw (Table 2: case 2) for **a** remaining dry matter (%DW), **b** lignin and **c** nitrogen concentrations of litter

model fit on nitrogen concentrations in particular, is low for any sample with an initial concentration of lignin<180 mg gDW^{-1}.

Qualitative behaviour of the model

An illustration of the mechanism how lignin concentration effects dynamics of microbial biomass nitrogen, dissolved organic nitrogen (DON) and nitrogen in the humus pool in our DECONIT model is given in Fig. 5. Based on experimental data from a laboratory study on decomposition of spruce needles and sheep laurel foliage (Joanisse et al., 2008) we varied the initial lignin pool or the initial total nitrogen concentration. Our simulation show, that the growth of microbial biomass and, thus the increase in microbial biomass nitrogen, is strongly affected by the initial lignin concentration. If DECONIT is initialised with twice as high total nitrogen contents but with measured lignin concentrations we simulate generally higher concentrations of inorganic nitrogen, an earlier timing of the offset of microbial growth and a more efficient accumulation of nitrogen in stable humus compounds (Fig. 5d). Under these conditions microbial growth in our model is carbon limited rather than nitrogen limited. A 50% reduction of initial lignin concentration (hence higher concentrations of labile compounds) on the other hand, lead to a very efficient incorporation of nitrogen into microbial tissue and initially, a slower accumulation of nitrogen in the humus. The optimum nitrogen concentration that remains enclosed in microbial tissue is much higher than for the other litter types, but decreases fast as the

labile compounds exhaust and carbon availability decreases. The quantity of nitrogen that is contained in humus, is very similar to the quantity that had accumulated in the humus with decomposition using measured values of tissue composition.

Q_{10} temperature dependency function

There is a vast amount of literature available on the use of a Van 't Hoff formulation for temperature dependencies. Davidson et al. (2006) for example, provide an excellent overview of problems that are associated with the use of empirical temperature dependency models. It is important to note that Davidson et al. (2006) questions not only the use of the van 't Hoff formulation, but the general concept of empirical temperature functions. A more process-based solution, however, will require measurements from a number of conditions that are scarcely followed in decomposition studies such as temperature dependencies of enzyme activity or half-optimum substrate concentrations (Davidson et al., 2006). Davidson et al. (2006) further claim that apparent Q_{10} values of respiration that are significantly above about 2.5 indicate that some unidentified process of substrate supply is confounded by the observed temperature variation.

Microbial growth and DOC dynamics

Our simulations showed a burst in microbial growth following an initial delay phase. Such behaviour agrees with findings of Parnas (1976), who succes-
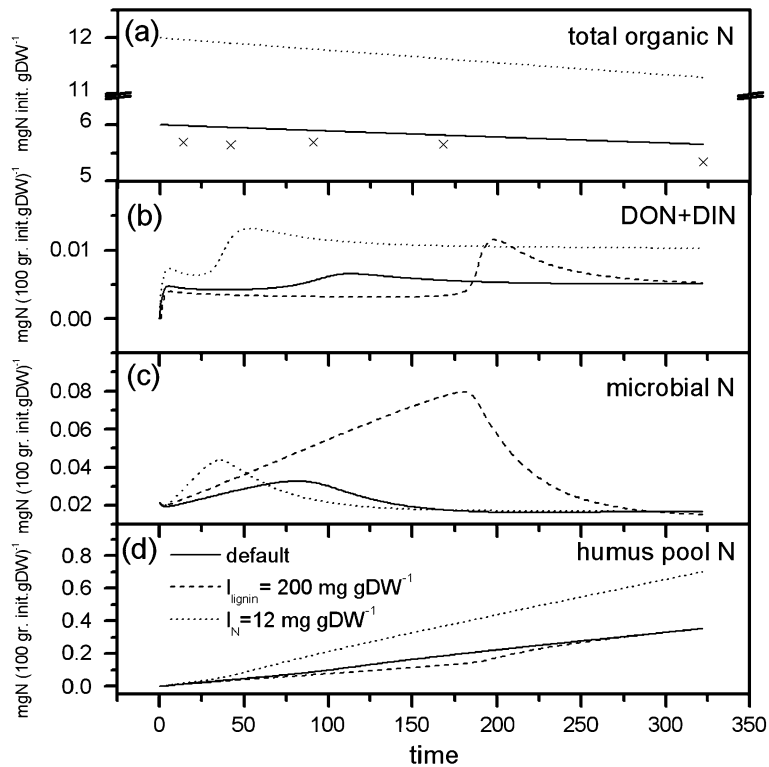
Fig. 5 Simulated decomposition dynamics of nitrogen compounds and microbial biomass nitrogen for black spruce needles and sheep laurel foliage under laboratory conditions (incubation Temperature: 20°C). For further information see Table 2 (case 52) and Joanisse et al. (2008). Shown are simulations using I.) measured lignin concentrations (solid line), II.) 50% of measured lignin concentrations (dashed line; I_{Lignin}=200 mg g DW^{-1}) and III.) assuming 200% of initial nitrogen content (dotted line; I_N=12 mg g DW^{-1}). **a** total organic nitrogen [crosses are measurements]; **b** dissolved organic nitrogen; **c** microbial nitrogen and **d** humus pool nitrogen

sively used the stoicheometric ratio (the required ratio for growth) of carbon and nitrogen, to predict the growth of *Escherichia coli* (wild type) microbes. Bursts of microbial activity have also been observed in a series of field experiments dealing with re-wetting of soils following prolonged drought periods (Davidson et al. 1991; García-Méndez et al. 1991; Butterbach-Bahl et al. 2004).

Related to the delay of microbial growth at the start of the experiments, which is in agreement with observations, is the simulated accumulation of DOC. Such accumulation contradicts the common ground assumption that labile carbon fluxes are fast and independent of temperature (for example Boddy et al. 2008). However, Rees et al. (2006) found increased leaching of DOC in the first stage of a decomposition experiment. They explained their findings with nitrogen-limited microbial growth hampering DOC immobilisation, i.e. in-line with our simulations. An issue worth some consideration is that DOC functions as a container concept that

includes a range of chemicals from lignocellulose-derivatives to sugars. Further consideration deserves also the use of a constant microbial C:N ratio. Frieder and Gabel (2001), for example found ranges from 4.0 to 12.0. Such tolerance could be ecologically significant as it prevents the substrates to accumulate.

Conclusion

We applied a new model of decomposition and nitrification to a comprehensive dataset of litter incubation experiments, including measurements of concentrations of lignin, cellulose, soluble carbon, microbial biomass, respiration, concentrations of DON and NH_4^+. The model draws from the assumption that nitrogen release is strongly related to the decomposition of lignin, and uses a complex Michaelis-Menten formulation to derive microbial growth rates from substrate concentrations.

The DECONIT model simulations show that carbon quality, expressed in initial concentrations of lignin and cellulose can be used to predict plant litter decomposition. However, the assumption that nitrogen mineralization is strongly linked with the decomposition of lignin only holds for tissues in which lignin concentrations exceed approximately 180 mg DW^{-1}. The model application to laboratory measurements of microbial biomass, respiration, DON and NH$_4^+$ was successful.

The application of the DECONIT model to a large set of field and laboratory decomposition experiments indicate the potential of our approach for describing decomposition processes and, thus, DECONIT may be a potentially attractive alternative for describing decomposition in complex biogeochemical ecosystem models.

References

Berg B, McClaugherty C (1978) Nitrogen release from litter in relation to the disappearance of lignin. Biogeochem. 4:219–224

Berg B, Booltink H et al (1991a) Data on needle litter decomposition and soil climate as well as site characteristics for some coniferous forest sites. Part 1. Site characteristics. Swedish University of Agricultural Sciences Department of Ecology and Environmental Research, Second edition report 41.

Berg B, Booltink H et al (1991b) Data on needle litter decomposition and soil climate as well as site characteristics for some coniferous forest sites. Part 2. Decomposition data. Swedish University of Agricultural Sciences Department of Ecology and Environmental Research, Second edition report 42

Berg B, Ekbohm G (1991) Litter mass—loss rates and decomposition patterns in some needle and leaf litter types. Long—term decomposition in a Scots pine forest. VII. Can. J. Bot. 69:1449–1456

Berg B, Berg MP et al (1993) Litter mass loss rates in pine forests of Europe and Eastern United States: some relationships with climate and litter quality. Biogeochem. 20:127–159

Berg B (2000) Litter decomposition and organic matter turnover in northern forest soils. For. Ecol. Man. 133 pp 13–22

Blagodatsky SA, Richter O (1998) Microbial growth in soil and nitrogen turnover: a theoretical model considering the activity state of microorganisms. Soil Biol Biochem 30:1743–1755

Blaney H F, Criddle W D, (1950) Determining water requirement in irrigated areas from climatological and irrigation data. USDA, SCS, SCS-TP96, 48p

Boddy E, Robberts P, Hill P W, Farrar J, Jones D L (2008) Turnover of low molecular weight dissolved organic C (DOC) and microbial C exhibit different temperature sensitivities in Arctic tundra soils. Soil Biol. Biochem. 40 1557–1566.

Braakhekke W, Bruijn AMG (2006) Modelling decomposition of standard plant material along an altitudinal gradient: a re-analyses of Coûteaux et al., (2002). Soil Biology and Biochem 39:99–105

Braswell BH, SacksWJ LE, Schimel DS (2005) Estimating diurnal to annual ecosystem parameters by synthesis of a carbon flux model with eddy covariance net ecosystem observations. Global Change Biol. 11:335–355

Butterbach-Bahl K, Kock M, Willibald G Hewett B, Buhagiar S, Papen H, Kiese R (2004) Temporal variations of fluxes of NO, NO$_2$, N$_2$O, CO$_2$ and CH$_4$ in a tropical rain forest ecosystem. Global Biogeochem. Cycl. 18(3). doi:101029/2004GB002243

Chen H, Harmon E, Griffiths RP, Hicks W (2000) Effects of temperature and moisture on carbon respired from decomposing woody roots. Forest Ecol. Managem. 138:51–61

Cooke RC, Whipps JM (1993) Ecophysiology of fungi. Blackwell, Oxford, UK

Cornwell WK, Cornelissen JHC et al (2008) Plant species traits are the predominant control over litter decomposition rates within biomes worldwide. Ecol. Letters 11:1065–1071

Cox PM, Betts RA, Jones CD et al (2000) Acceleration of global warming due to carbon-cycle feedbacks in a coupled climate model. Nature 408:184–187

Coûteaux MM, Bottner P, Berg B (1995) Litter decomposition, climate and litter quality. Trends Ecol Evol 10:63–66

Coûteaux MM, Sarmiento L, Bottner P, Acevedo D, Thiéry JM, Vallejo VR (2002) Decomposition of standard plant material along an altitudinal transect (65–3968 m) in the tropical Andes. Soil Biol Biochem 34:69–78

Davidson EA, Vitousek PM, Matson PA, Riley R, Garciá-Méndez G, Maass JM (1991) Soil emissions of nitric oxide in a seasonally dry tropical forest of México. J. Geophys. Res. 96:15439–15445

Davidson EA, Janssens IA, Luo I (2006) On the variability of respiration in terrestrial ecosystems: moving beyond Q10. Global Change Biol. 12:154–164

Davidson EA, Janssens IA (2006) Temperature sensitivity of soil carbon decomposition and feedbacks to climate change. Nature 440:165–173

Fioretto A, Di Nardo C, Papa S, Fuggi A (2005) Lignin and cellulose degradation and nitrogen dynamics during decomposition of three litter species in a Mediterranean ecosystem Soil Biol. Biochem. 37:1083–1091

Frieder JK, Gabel D (2001) Microbial biomass and microbial C:N ratio in bulk soil and buried bags for evaluating in situ net N mineralization in agricultural soils. J. Plant Nutr. Soil Sci. 164:673–679

García-Méndez G, Maass JM, Matson P, Vitousek PM (1991) Nitrogen transformations and nitrogen oxide flux in tropical deciduous forest in México. Oecologia 88:362–3

Henriksen TM, Breland TA (1999) Decomposition of crop residues in the field: evaluation of a simulation model developed from microcosm studies. Soil Biol Biochem 31:1423–1434

Houghton RA, Davidson EA, Woodwell GM (1998) Missing sinks, feedbacks, and understanding the role of terrestrial ecosystems in the global carbon balance. Global Biogeochem. Cycl. 12:25–34

IPCC (2007) Summary for Policymakers. Climate Change 2007: The Physical Science Basis. Contribution of Working Group I to the Fourth Assessment Report of the Intergovernmental Panel on Climate Change. In: Solomon S, Qin D, Manning M, Chen Z, Marquis M, Averyt KB, Tignor M, Miller HL (eds) Cambridge University Press. Cambridge, United Kingdom and New York, NY, USA

Jansson PE, Karlberg L (2004) Coupled heat and mass transfer model for soil-plant-atmosphere systems. Royal Institute of Technology, dept of Civil and Environmental Engeneering, Stockholm, 435 (www.lwr.kth.se/CoupModel/CoupModel.pdf)

Joanisse GD, Bradley RL, Preston CM (2008) Do late-successional tannin-rich plant communities occurring on high acidic soils increase the DON/DIN ratio? Biol Fertil Soils 44:903–907

Kirschbaum MUF (1995) The temperature dependence of soil organic matter decomposition and the effect of global warming on soil organic C storage, Soil Biol. Biochem. 27:753–760

Kirschbaum MUF (2000) Will changes in soil organic carbon act as a positive or negative feedback on global warming? Biogeochemistry 48:21–50

Leffelaar PA, Wessel WW (1988) Denitrification in a homogeneous, closed system: experiment and simulation. Soil Sci 146:335–349

Lenton TM, Huntingford C (2003) Global terrestrial carbon storage and uncertainties in its temperature sensitivity examined with a simple model. Global Change Biology 9:1333–1352

Li CS, Frolking S, Frolking TA (1992) A model of nitrous oxide evolution from soil driven by rainfall events, 1, Model structure and sensitivity. J. Geophys. Res. 97:9759–9776

Li C, Aber J, Stange F, Butterbach-Bahl K, Papen H (2000) A process-oriented model of N_2O and NO emissions from forest soils: 1, Model development. J. Geophys. Res. 105:4369–4384

Lohmander A, Kätterer T, Andrén O (1998) Modelling the effects of temperature and moisture on CO2 evolution from top- and subsoil using a multicomponent approach. Soil Biol Biochem 30:2023–2030

Lohmus K, Ivask M (1995) Decomposition and nitrogen dynamics of fine roots of Norway sprucs (Picea abies (L.) Karst.). Plant Soi 168–169:89–95 1995

Metropolis N, Rosenbluth AW, Rosenbluth MN et al (1953) Equations of state calculations by fast computing machines. J. Chem. Phys 21:1087–1092

Parnas H (1976) A theoretical explanation of the priming effect based on microbial growth with two limiting substrates. Soil Biol Biochem 8:139–144

Parton WJ, Hartman M, Oijima D, Schimel D (1998) DAYCENT and its land surface submodel: description and testing. Global Planet Change 19:35–48

Prentice IC, Farquhar GD, Fasham MJR et al (2001) The carbon cycle and atmospheric carbon dioxide. In: Houghton JT, Ding Y, Griggs DJ (eds) Climate Change 2001: The Scientific Basis. Cambridge University Press, Cambridge, UK, pp 183–237

Raich JW, Schlesinger WH (1992) The global carbon dioxide flux in soil respiration and its relationship to vegetation and climate. Tellus 44B:81–89

Rees R, Change SC, Wang CP, Matzner E (2006) Release of nutrients and dissolved organic carbon during decomposition of Chamaecyparis obtusa var. formosana leaves in a mountain forest in Taiwan. J. Plant Nutr. Soil Sci 169:792–798

Roberts DV (1977) Enzyme kinetics. Cambridge University Press, Cambridge

Schimel JP, Weintraub MN (2003) The implications of exoenzyme activity on microbial carbon and nitrogen limitation in soil: a theoretical model. Soil Biol Biochem 35:549–563

Shah DB, Coulman GA (1978) Kinetics of nitrification and denitrification reactions, Biotechn. Bioengin. 20:43–72

Sitch S, Huntingford C, Gedney N, Levy PE, Lomas M, Piao SL, Betts R, Ciais P, Cox P, Friedlingstein P, Jones CD, Prentice IC, Woodward FI (2008) Evaluation of the terrestrial carbon cycle, future plant geography and climate-carbon cycle feedbacks using five Dynamic Global Vegetation Models (DGVMs). Global Change Biol 14:2015–2039

Van Oijen M, Rougier J, Smith R (2005) Bayesian calibration of process-based forest models: bridging the gap between models and data. Tree Phys. 25:915–927

Wessén B, Berg B (1986) Long-term decomposition of barley straw: chemical changes and ingrowth of fungal mycelium. Soil Biol Biochem 18:53–59

Wang H, Curtin D, Jame YW, McConkey BG, Zhou HF (2002) Simulation of soil carbon dioxide flux during plant residue decomposition. S. Sci. Soc. Am. J. 66:1304–1310

Whitmore AP (1991) A method for assessing the goodness of computer simulation of soil processes. J. Soil Sci. 42:289–299

Zobith JM, Moore DJP, Sacks WJ, Monson RK, Bowling DR, Schimel DS (2008) Integration of process-based soil respiration models with whole ecosystem CO_2 measurements. Ecosystems 11:250–269